# Model Predictive Control for Modeling and Simulation of Human Gait Motions

**Vu Trieu Minh*[a1], Mart Tamre [b1], Victor Musalimov [c2], Pavel Kovalenko [d2], Irina Rubinshtein [e2], Ivan Ovchinnikov [f2], Reza Moezzi [g3]**

[1]Department of Electrical Power Engineering and Mechatronics
Tallinn University of Technology, Estonia
[2]Department of Mechatronics,
Saint Petersburg State University of Information Technologies, Mechanics and Optics, Russia
[3]Institute for Nanomaterials, Advanced Technologies and Innovation
Technical University of Liberec, Czech Republic
*Corresponding author
*[a]trieu.vu@ttu.ee, [b]mart.tamre@ttu.ee, [c]musvm@yandex.ru, [d]ovalenko_p.p@mail.ru,
[e]rubinshteiniv@gmail.com, [f]ovi2745@mail.ru, [g]reza.moezzi@tul.cz

## ABSTRACT

Human motion is a complex activity of the central nervous system (CNS) and muscles. Performance of a human motion can be decomposed into three components: estimation of trajectory; calculation of required signal for muscles; and performance of movement. The CNS conducts the first two tasks and the muscles perform the third task. This paper presents the development of a mathematical model and a Matlab Simulink plant for human gait movement. An internal model predictive control (MPC) is setup and plays as the human CNS to estimate the trajectory and to calculate the required signal for muscles to perform the movement. MPC calculates the required torques for each joint and generate optimal trajectories subject to human physical constraints for muscles. Results of simulation are analyzed and compared to the real human gait motions captured by a real motion capture system (Vicon). Finally, conclusions and recommendations from this research are withdrawn.

*Keywords:* Human gait model; human gait plant; central nervous system; model predictive control; 5-link mechanism; motion capture system.

## 1. INTRODUCTION

Human movements are performed simultaneously by the central nervous system (CNS), muscles, and limbs. Recently, there are many researches on modeling human gait motions for mimicking the real human trajectories as well as the walking patterns, despite the fact that, each person has its owned gait motion or the gait of each person is unique. Most of design and development of human gait are based on the intuition, followed by experimental verifications. These approaches are usually costly, unsustainable and ineffective.

Modeling human gait motion is interested by researchers since the gait simulations can be used to identify individuals by their gait for security systems similar to the

human scan fingerprints, retina and face unlock. In medicine, modeling human gait can be used to detect various disorders and abnormalities of the musculoskeletal system. Medicine doctor can check his/her assumptions about a disease of limbs without costly tests on patients. Human gait modeling can also help to simplify the process to test orthotic devices and artificial limbs since these devices are normally tested empirically and expensively.

This study aims to develop a simple and flexible solution for modeling and simulation of the human gait used MPC algorithms. MPC plays as the human CNS to generate the required torques and optimal trajectories for muscles. MPC allows solving online the optimal solution subject to constraints from inputs and outputs. In this paper, MPC algorithms are developed as in Minh V.T., Afzulpurkar N., 2005 [1], which allows guaranteeing stability of the system in presence of the plant-model errors and uncertainties. A human gait model based on a kinematics of human body from data achieved from a camera of optoelectronic system for measuring three dimensions is developed in Vergallo P., *et al.*, 2015 [2], where sophisticated software are used to convert the images of human walking based on appropriate protocols to describe the human motions in each joint. Another human gait model used the biomechanical principles of Lagrange method for reproducing the properties of human walking is presented in Luengas L.A., *et al.*, 2015 [3], where anthropometric data are used to simulate the human walking dynamics. Comparisons of the model simulations and the real camera measurements show that the model can reproduce accurate characteristics of the gait motions.

Several approaches involving the use of three dimensional cameras and image processing have been introduced. However in Gill T., *et al.*, 2011 [4], a less expensive method for using the infrared depth camera for modeling the human gait is presented in spaces with low or no light conditions with passive sensors. The cost for this method is low but the advantages and precision of this method are still unclear.

A PhD dissertation on dynamic modeling of human gait using model predictive control approach is presented in Sun J., 2015 [5], where a plant model for the human gait dynamics is built and a control feedback with PID and MPC is designed for simulating the human gait. This control method provides unlimited flexible gaits. However the disadvantage of this method is unable to ensure the stability and robustness of the system.

Most of numerical researches are used the Lagrange equations to describe the motions of limbs and modeling the gaits as 5-link, 7-link, or 9-link mechanism. However, there are limitations from those methods that they are unable to include the constraints of dynamic equations such as the constraints for joint torques, angles, mass centers. For example, in Ren L., *et al.*, 2006 [6], some good results, which are almost matching the experimental data, are achieved, but paths of some point motions are totally incorrect and the computations are very complicated. Therefore, in Ren L., *et al.*, 2007 [7], a predictive modeling of human walking over a complete gait is presented. The disadvantages of this reference are the lack of constrained conditions and the failure to develop an objective function that is able to minimize the energy cost.

A completed control function for arm swing and human walking is developed in Pontzer H., et al., 2009 [8] with an assumption that the arm acts as a passive mass damper and powered by the movement of the human lower body. While Mohammed S, et al., 2016 [9] develop the recognition of gaits using wearable sensors, this reference monitors the human walking through the analysis of the human center of force and predicts any abnormal walking pattern. Identification of different gaits is detected from characteristics of gait phases.

In our research, a mathematic model describing the movement of anthropomorphic mechanism is developed, which is close (but not sufficient) to the real plant. Then, MPC algorithms are developed to calculate the required toques for muscles. It is assumed that the human walking is a 5-link mechanism and the CNS is to predict and calculate the lower extremities (feet, shins, hips, and body) to perform the human movements. MPC algorithms for nonlinear models and different MPC computational schemes are referred in Minh V.T., Afzulpurkar N., 2006 [10], where nonlinear MPC with zero terminals and nonlinear NMPC with softened state constraints are developed and compared. For setting up a human plant, some mechanical blocks in Minh V.T., Rashid A.A., 2012 [11] are used in Matlab Simulink. Latest references on model predictive control and human gait simulation are referred to in [12], [13], [14], [15], [16], [17], [18], [19], and [20].

The structure of this paper is as follows: Section 2 presents the mathematical modelling; Section 3 describes the experimental data collection; Section 4 designs MPC controller; Section 5 designs the plant model; Section 6 illustrates results of simulation; and finally conclusions and recommendations are withdrawn in section 7.

## 2. MATHEMATICAL MODEL

The mathematical model of a human 5-link mechanism is shown in figure 1. This model is used for MPC to calculate the optimal torques at each joint. Five weighty links are *OC*, *OB*, *OD*, *DE*, and *BE*. Link *OC* is the body. *ODE* and *OBA* are feet. Each leg consists of the thigh and lower leg, so that the link *OB* and *OD* are hips and units *BA* and *DE* are shins. Two legs are considered of the same weight and length.
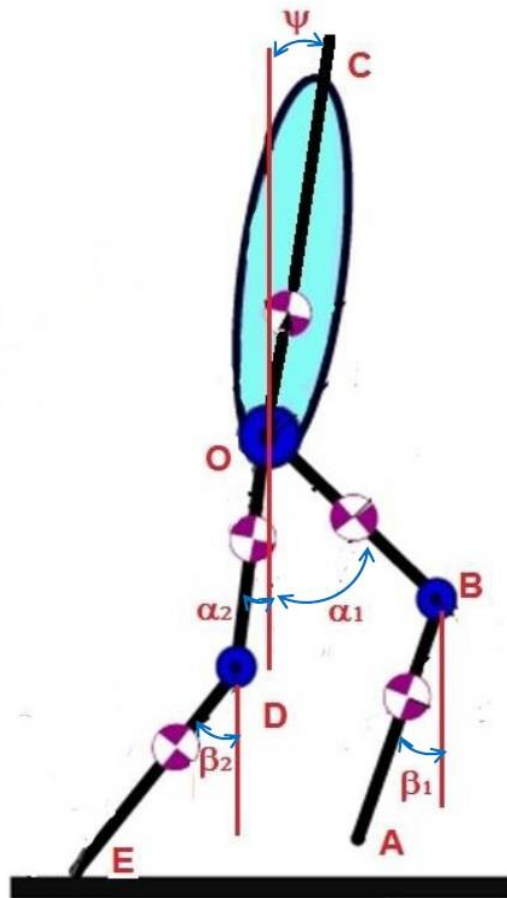


Figure 1. Model of 5-link mechanism

Joint $O$ connecting the body $OC$ with hips $OB$ and $OD$ is referred as hip joint, joints $B$ and $D$, connecting the thigh $OB$ and $OD$ with shins $BA$ and $DE$, are referred as knee joints. All joints are assumed to be ideal, i.e. the friction is neglected. This mechanism is consisted of seven degrees of freedom with coordinates $x$, $y$ of hip $O$ and five angles $\psi$, $\alpha_1$, $\alpha_2$, $\beta_1$, $\beta_2$, between the links and the vertical.

In 5-link model, we assume that the feet do not have strong influence to the movement of other parts of human. Then, the feet are excluded from this model. The following equations are used for calculation.

Lagrange equation:

$$\frac{d}{dt} \cdot \frac{\partial L}{\partial \dot{q}_i} - \frac{\partial L}{\partial q_i} = Q_s \tag{1}$$

where $Q_s$ – generalizes non conservative force, and

$$L = T - V \tag{2}$$

where $L$ – Lagrangian; $T$ – kinetic energy; $V$ – potential energy;

Kinetic energy:

$$T = \frac{1}{2}(mv^2 + 2m(v\omega)p + \Theta\omega^2) \tag{3}$$

where, $m$ – mass of link; $v$ – absolute velocity; $\nu$ – pole velocity; $\omega$ – angular velocity; $p$ – radius vector of the center of mass; $\Theta$ – Inertia moment relative to pole.

$$\nu = \begin{pmatrix} \dot{x} \\ \dot{y} \\ 0 \end{pmatrix} \tag{4}$$

$$\omega = \dot{\psi}\begin{pmatrix} sin(\psi) \\ cos(\psi) \\ 0 \end{pmatrix} \tag{5}$$

Kinetic energy of link $OC$:

$$T_{OC} = \frac{1}{2}\left(m_k(\dot{x}^2 + \dot{y}^2) - 2K_r\dot{\psi}(\dot{x}\,cos(\psi) + \dot{y}\,sin(\psi)) + J\dot{\psi}^2\right) \tag{6}$$

where $K_r = m_k r$; $m_k$ – Mass $OC$; $r$ – distance from $O$ to $OC$ mass centre; $J$ – inertia moment $OC$ relative to point $O$.

Kinetic energy of link $OB$:

$$T_{OB} = \frac{1}{2}\left(m_a(\dot{x}^2 + \dot{y}^2) + 2m_a a\dot{\alpha}_1(\dot{x}\,cos(\alpha_1) + \dot{y}\,sin(\alpha_1)) + J_a^0\dot{\alpha}_1^2\right) \tag{7}$$

where $m_a$ – mass $OB$; $a$ – distance from $O$ to $OB$ mass centre; $J_a^0$ – inertia moment $OB$ relative to point $O$.

Kinetic energy of link $BA$:

$$T_{BA} = \frac{1}{2}\Big(m_b\big(\dot{x}^2 + \dot{y}^2 + 2\dot{\alpha}_1 L_a(\dot{x}\,cos(\alpha_1) + \dot{y}\,sin(\alpha_1)) + L_a^2\dot{\alpha}_1^2\big) + 2K_b\dot{\beta}_1(\dot{x}\,cos(\beta_1) + \dot{y}\,sin(\beta_1)) + J_b\dot{\beta}_1^2\Big) \tag{8}$$

where $K_b = m_b b$; $m_b$ – mass $BA$; $b$ – distance from $B$ to $BA$ mass centre; $L_a$ – length of $OB$; $J_b$ – inertia moment $BA$ relative to point $B$.

$T_{OD}$ and $T_{DE}$ are similar to $T_{OB}$ and $T_{BA}$ by changing the indexes from 1 to 2. Then, the Kinetic energy:

$$T = T_{OC} + T_{OB} + T_{BA} + T_{OD} + T_{DE} = \frac{1}{2}M(\dot{x}^2 + \dot{y}^2) + \frac{1}{2}J\dot{\psi}^2 - K_r\dot{\psi}(\dot{x}\,cos(\psi) + \dot{y}\,sin(\psi)) + \sum_{i=1}^{2}\left[\frac{1}{2}J_a\dot{\alpha}_i^2 + \frac{1}{2}J_b\dot{\beta}_i^2 + K_a\dot{\alpha}_i(\dot{x}\,cos(\alpha_i) + \dot{y}\,sin(\alpha_i)) + K_b\dot{\beta}_i(\dot{x}\,cos(\beta_i) + \dot{y}\,sin(\beta_i)) + J_{ab}\dot{\alpha}_i\dot{\beta}_i\,cos(\alpha_i - \beta_i)\right] \tag{9}$$

where:

$$M = m_k + 2m_a + 2m_b - total\ mass \tag{10}$$

$$K_a = m_a a + m_b L_a \tag{11}$$

$$J_a = J_a^0 + m_b L_a^2 \tag{12}$$

$$J_{ab} = K_b L_a = m_b b L_a \tag{13}$$

Potential energy:

$$V = g\big[m_k(y + r\cos(\psi)) + \sum_{i=1}^{2}(m_a(y - a\cos(\alpha_i)) + m_b(y - L_a\cos(\alpha_i) - b\cos(\beta_i)))\big] = g[My + K_r\cos(\psi) - \sum_{i=1}^{2}(K_a\cos(\alpha_i) + K_b\cos(\beta_i))] \tag{14}$$

In this paper, MPC algorithms are used to find the optimal trajectory based on the minimization of an objective function and subject to constraints. Therefore, from equation (1), we find $T$ and $V$, next we need to find $Q_s$ by the following equations:

$$\delta W = (R_{1x} + R_{2x})\delta x + (R_{1y} + R_{2y})\delta y - (q_1 + q_2)\delta\psi + \sum_{i=1}^{2}\big[(q_i - u_i)\delta\alpha_i + (u_i - P_i)\delta\beta_i + R_{1x}\delta(L_a\sin(\alpha_i) + L_b\sin(\beta_i)) - R_{1y}\delta(L_a\cos(\alpha_i) + L_b\cos(\beta_i))\big] = \sum_{i=1}^{2}\big[R_{ix}\delta x + R_{iy}\delta y - q_i\delta\psi + (q_i - u_i + R_{1x}L_a\cos(\alpha_i) + R_{1y}L_a\sin(\alpha_i))\delta\alpha_i + (u_i - P_i + R_{1x}L_b\cos(\beta_i) + R_{1y}L_b\sin(\beta_i))\delta\beta_i\big] \tag{15}$$

where,

$$Q_x = R_{1x} + R_{2x} \tag{16}$$

$$Q_y = R_{1y} + R_{2y} \tag{17}$$

$$Q_\psi = -q_1 - q_2 \tag{18}$$

$$Q_{\alpha_1} = q_1 - u_1 + R_{1x}L_a\cos(\alpha_1) + R_{1y}L_a\sin(\alpha_1) \tag{19}$$

$$Q_{\alpha_2} = q_2 - u_2 + R_{1x}L_a\cos(\alpha_2) + R_{1y}L_a\sin(\alpha_2) \tag{20}$$

$$Q_{\beta_1} = u_1 - P_1 + R_{1x}L_b\cos(\beta_1) + R_{1y}L_b\sin(\beta_1) \tag{21}$$

$$Q_{\beta_2} = u_2 - P_2 + R_{1x}L_b\cos(\beta_2) + R_{1y}L_b\sin(\beta_2) \tag{22}$$

The derivatives of these variables can be written as follows:

Derivative $\frac{\partial L}{\partial z}$ :

$$\frac{\partial L}{\partial x} = \frac{\partial(T - V)}{\partial x} = 0 \tag{23}$$

$$\frac{\partial L}{\partial y} = \frac{\partial(T - V)}{\partial y} = -gM \tag{24}$$

$$\frac{\partial L}{\partial\psi} = \frac{\partial(T-V)}{\partial\psi} = K_r\big(\dot{x}\dot{\psi}\sin(\psi) - \dot{y}\dot{\psi}\cos(\psi) - g\sin(\psi)\big) \tag{25}$$

$$\frac{\partial L}{\partial\alpha_i} = \frac{\partial(T-V)}{\partial\alpha_i} = K_a(\dot{\alpha}_i\dot{x}\sin(\alpha_i) - \dot{\alpha}_i\dot{y}\cos(\alpha_i) + g\sin(\alpha_i)) - J_{ab}\dot{\alpha}_i\dot{\beta}_i\sin(\alpha_i - \beta_i) \tag{26}$$

$$\frac{\partial L}{\partial\beta_i} = \frac{\partial(T-V)}{\partial\beta_i} = K_b\big(\dot{\beta}_i\dot{x}\sin(\beta_i) - \dot{\beta}_i\dot{y}\cos(\beta_i) + g\sin(\beta_i)\big) - J_{ab}\dot{\alpha}_i\dot{\beta}_i\sin(\alpha_i - \beta_i) \tag{27}$$

Derivative $\frac{\partial L}{\partial\dot{z}}$ :

$$\frac{\partial L}{\partial\dot{x}} = M\dot{x} - K_r\dot{\psi}\cos(\psi) + K_a\dot{\alpha}_i\cos(\alpha_i) + K_b\dot{\beta}_i\cos(\beta_i) \tag{28}$$

$$\frac{\partial L}{\partial\dot{y}} = M\dot{y} - K_r\dot{\psi}\sin(\psi) + K_a\dot{\alpha}_i\sin(\alpha_i) + K_b\dot{\beta}_i\sin(\beta_i) \tag{29}$$

$$\frac{\partial L}{\partial \dot{\psi}} = J\dot{\psi} - K_r(\dot{x}\cos(\psi) + \dot{y}\sin(\psi)) \tag{30}$$

$$\frac{\partial L}{\partial \dot{\alpha}_i} = J_a\dot{\alpha}_i + K_a(\dot{x}\cos(\alpha_i) + \dot{y}\sin(\alpha_i)) + J_{ab}\dot{\beta}_i\cos(\alpha_i\text{-}\beta_i) \tag{31}$$

$$\frac{\partial L}{\partial \dot{\beta}_i} = J_b\dot{\beta}_i + K_b(\dot{x}\cos(\beta_i) + \dot{y}\sin(\beta_i)) + J_{ab}\dot{\alpha}_i\cos(\alpha_i\text{-}\beta_i) \tag{32}$$

Derivatives: $\frac{d}{dt}\frac{\partial L}{\partial \dot{z}}$:

$$\frac{d}{dt}\frac{\partial L}{\partial \dot{x}} = M\ddot{x} - K_r\ddot{\psi}\cos(\psi) + K_r\dot{\psi}^2\sin(\psi) + K_a\ddot{\alpha}_i\cos(\alpha_i) - K_a\dot{\alpha}_i{}^2\sin(\alpha_i) +$$
$$K_b\ddot{\beta}_i\cos(\beta_i) - K_b\dot{\beta}_i{}^2\sin(\beta_i) \tag{33}$$

$$\frac{d}{dt}\frac{\partial L}{\partial \dot{y}} = M\ddot{y} - K_r\ddot{\psi}\sin(\psi) - K_r\dot{\psi}^2\cos(\psi) + K_a\ddot{\alpha}_i\sin(\alpha_i) + K_a\dot{\alpha}_i{}^2\cos(\alpha_i) +$$
$$K_b\ddot{\beta}_i\sin(\beta_i) + K_b\dot{\beta}_i{}^2\cos(\beta_i) \tag{34}$$

$$\frac{d}{dt}\frac{\partial L}{\partial \dot{\psi}} = J\ddot{\psi} - K_r(\ddot{x}\cos(\psi) + \ddot{y}\sin(\psi) - \dot{x}\dot{\psi}\sin(\psi) + \dot{y}\dot{\psi}\cos(\psi)) \tag{35}$$

$$\frac{d}{dt}\frac{\partial L}{\partial \dot{\alpha}_i} = J_a\ddot{\alpha}_i + K_a(\ddot{x}\cos(\alpha_i) + \ddot{y}\sin(\alpha_i) + \dot{x}\dot{\alpha}_i\sin(\alpha_i) - \dot{y}\dot{\alpha}_i\cos(\alpha_i)) +$$
$$J_{ab}\ddot{\beta}_i\cos(\alpha_i - \beta_i) - J_{ab}\dot{\beta}_i(\alpha_i - \beta_i)\sin(\alpha_i - \beta_i) \tag{36}$$

$$\frac{d}{dt}\frac{\partial L}{\partial \dot{\beta}_i} = J_b\ddot{\beta}_i + K_b(\ddot{x}\cos(\beta_i) + \ddot{y}\sin(\beta_i) + \dot{x}\beta_i\sin(\beta_i) - \dot{y}\beta_i\cos(\beta_i)) +$$
$$J_{ab}\ddot{\alpha}_i\cos(\alpha_i - \beta_i) - J_{ab}\dot{\alpha}_i(\dot{\alpha}_i - \beta_i)\sin(\alpha_i - \beta_i) \tag{37}$$

Finally, the full Lagrange equations for this 5–link mechanism are:

$$M\ddot{x} - K_r\ddot{\psi}\cos(\psi) + K_r\dot{\psi}^2\sin(\psi) + K_a\ddot{\alpha}_i\cos(\alpha_i) - K_a\dot{\alpha}_i{}^2\sin(\alpha_i) +$$
$$K_b\ddot{\beta}_i\cos(\beta_i) - K_b\dot{\beta}_i{}^2\sin(\beta_i) = R_{1x} + R_{2x}, \quad (i = 1,2) \tag{38}$$

$$M\ddot{y} - K_r\ddot{\psi}\sin(\psi) - K_r\dot{\psi}^2\cos(\psi) + K_a\ddot{\alpha}_i\sin(\alpha_i) + K_a\dot{\alpha}_i{}^2\cos(\alpha_i) +$$
$$K_b\ddot{\beta}_i\sin(\beta_i) + K_b\dot{\beta}_i{}^2\cos(\beta_i) = R_{1y} + R_{2y} - Mg, \quad (i = 1,2) \tag{39}$$

$$-K_r\ddot{x}\cos(\psi) - K_r\ddot{y}\sin(\psi) + J\ddot{\psi} - K_r g\sin(\psi) = -q_1 - q_2, \quad (i = 1,2) \tag{40}$$

$$K_a\ddot{x}\cos(\alpha_i) + K_a\ddot{y}\sin(\alpha_i) + J_a\ddot{\alpha}_i + J_{ab}\ddot{\beta}_i\cos(\alpha_i - \beta_i) + J_{ab}\dot{\beta}_i{}^2\sin(\alpha_i - \beta_i) + K_a\,g\sin(\alpha_i) = q_i - u_i + R_{1x}L_a\cos(\alpha_i) + R_{1y}L_a\sin(\alpha_i), \quad (i = 1,2); \tag{41}$$

$$K_b\ddot{x}\cos(\beta_i) + K_b\ddot{y}\sin(\beta_i) + J_b\ddot{\beta}_i + J_{ab}\ddot{\alpha}_i\cos(\alpha_i - \beta_i) - J_{ab}\dot{\alpha}_i{}^2\sin(\alpha_i - \beta_i) + K_b\,g\sin(\beta_i) = u_i - P_i + R_{1x}L_b\cos(\beta_i) + R_{1y}L_b\sin(\beta_i), \quad (i = 1,2) \tag{42}$$

This model has constrained movement as point *A* and *E* for being fixed on the ground surface. When point *A* is fixed on the ground surface, we have the kinematic equations for *x* and *y*:

$$x = x_A - L_a\sin(\alpha_1) - L_b\sin(\beta_1) \tag{43}$$
$$y = y_A + L_a\cos(\alpha_1) + L_b\cos(\beta_1) \tag{44}$$
$$\dot{x} = -L_a\dot{\alpha}_1\cos(\alpha_1) - L_b\dot{\beta}_1\cos(\beta_1) \tag{45}$$
$$\dot{y} = -L_a\dot{\alpha}_1\sin(\alpha_1) - L_b\dot{\beta}_1\sin(\beta_1) \tag{46}$$

Then, new equations for *T*, *V* and $\delta W$ from (9 to 14) using (43 to 46):

$$T = \frac{1}{2}J\dot{\psi}^2 + \frac{1}{2}M(J_a - 2L_aK_a + L_a{}^2M)\dot{\alpha}_1{}^2 + \frac{1}{2}J_a\dot{\alpha}_2{}^2 + \frac{1}{2}M(J_b - 2L_bK_b +$$
$$L_b{}^2M)\dot{\beta}_1{}^2 + \frac{1}{2}J_a\dot{\beta}_2{}^2 + L_aK_r\cos(\psi - \alpha_1)\dot{\psi}\dot{\alpha}_1 + L_bK_r\cos(\psi - \beta_1)\dot{\psi}\dot{\beta}_1 -$$
$$L_aK_a\cos(\alpha_1 - \alpha_2)\dot{\alpha}_1\dot{\alpha}_2 + (J_{ab} - L_aK_b - L_bK_a + L_aL_bM)\cos(\alpha_1 -$$
$$\beta_1)\dot{\alpha}_1\dot{\beta}_1 - L_aK_b\cos(\alpha_1 - \beta_2)\dot{\alpha}_1\dot{\beta}_2 - L_bK_a\cos(\alpha_2 - \beta_1)\dot{\alpha}_2\dot{\beta}_1 +$$
$$L_bK_b\cos(\beta_1 - \beta_2)\dot{\beta}_1\dot{\beta}_2 \tag{47}$$

$$V = g[My_A + K_r\cos(\psi) + (L_aM - K_a)\cos(\alpha_1) - K_a\cos(\alpha_2) + \tag{48}$$

$$(L_bM - K_b)\cos(\beta_1) - K_b\cos(\beta_2)]$$
$$\delta W = -(q_1 + q_2)\delta\psi + \left(q_1 - u_1 - R_{2x}L_a\cos(\alpha_1) - R_{2y}L_a\sin(\alpha_1)\right)\delta\alpha_1 +$$
$$\left(q_2 - u_2 - R_{2x}L_a\cos(\alpha_2) - R_{2y}L_a\sin(\alpha_2)\right)\delta\alpha_2 + \left(u_1 - P_1 - \right.$$
$$R_{2x}L_b\cos(\beta_1) - R_{2y}L_b\sin(\beta_1)\right)\delta\beta_1 + \left(u_2 - P_2 - R_{2x}L_b\cos(\beta_2) - \right.$$
$$\left. R_{2y}L_b\sin(\beta_2)\right)\delta\beta_2$$

(49)

These equations can be transformed into the matrix forms:

$$B_l\ddot{z}_l + gA\sin(z_i) + D(z)\dot{z}_l{}^2 = C(z)\omega \tag{50}$$

where $z_i = \begin{bmatrix}\psi\\\alpha_1\\\alpha_2\\\beta_1\\\beta_2\end{bmatrix}$, $\sin(z_i) = \begin{bmatrix}\sin\psi\\\sin\alpha_1\\\sin\alpha_2\\\sin\beta_1\\\sin\beta_2\end{bmatrix}$, $\dot{z}_l{}^2 = \begin{bmatrix}\dot{\psi}^2\\\dot{\alpha_1}^2\\\dot{\alpha_2}^2\\\dot{\beta_1}^2\\\dot{\beta_2}^2\end{bmatrix}$, $\omega = \begin{bmatrix}u_1\\u_2\\q_1\\q_2\\P_1\\P_2\\R_{2x}\\R_{2y}\end{bmatrix}$.

$$T = T(z,\dot{z}) = \frac{1}{2}\dot{z}B(z)\dot{z} \tag{51}$$

where,

$$B(z) = \begin{bmatrix}
J & L_aK_r\cos(\psi\text{-}\alpha_1) & 0 & L_bK_r\cos(\psi\text{-}\beta_1) & 0 \\
L_aK_r\cos(\psi\text{-}\alpha_1) & J_a\text{-}2L_aK_a\text{+}L_a{}^2M & -L_aK_a\cos(\alpha_1\text{-}\alpha_2) & (J_{ab}\text{-}L_aK_b\text{-}L_bK_a\text{+}L_aL_bM)\cos(\alpha_1\text{-}\beta_1) & -L_aK_b\cos(\alpha_1\text{-}\beta_2) \\
0 & -L_aK_a\cos(\alpha_1\text{-}\alpha_2) & J_a & -L_bK_a\cos(\alpha_2\text{-}\beta_1) & J_{ab}\cos(\alpha_2\text{-}\beta_2) \\
L_bK_r\cos(\psi\text{-}\beta_1) & (J_{ab}\text{-}L_aK_b\text{-}L_bK_a\text{+}L_aL_bM)\cos(\alpha_1\text{-}\beta_1) & -L_bK_a\cos(\alpha_2\text{-}\beta_1) & J_b\text{-}2L_bK_b\text{+}L_b{}^2M & -L_bK_b\cos(\beta_1\text{-}\beta_2) \\
0 & -L_aK_b\cos(\alpha_1\text{-}\beta_2) & J_{ab}\cos(\alpha_2\text{-}\beta_2) & -L_bK_b\cos(\beta_1\text{-}\beta_2) & J_b
\end{bmatrix}$$

And

$$V = V(z) = \dot{g}(My_A - \textstyle\sum_{i=1}^{5}a_{ii}\cos z_i) \tag{52}$$

where $a_{ii}$ are diagonal elements of $A$:

$$A = \begin{bmatrix}
-K_r & 0 & 0 & 0 & 0 \\
0 & K_a - L_aM & 0 & 0 & 0 \\
0 & 0 & K_a & 0 & 0 \\
0 & 0 & 0 & K_b - L_bM & 0 \\
0 & 0 & 0 & 0 & K_b
\end{bmatrix}$$

$D(z)$ is skew-symmetric matrix $d_{ij}(z) = -d_{ji}(z)$:

$$D(z) = \begin{bmatrix}
0 & L_aK_r\sin(\psi\text{-}\alpha_1) & 0 & L_bK_r\sin(\psi\text{-}\beta_1) & 0 \\
-L_aK_r\sin(\psi\text{-}\alpha_1) & 0 & -L_aK_a\sin(\alpha_1\text{-}\alpha_2) & (J_{ab}\text{-}L_aK_b\text{-}L_bK_a\text{+}L_aL_bM)\sin(\alpha_1\text{-}\beta_1) & -L_aK_b\sin(\alpha_1\text{-}\beta_2) \\
0 & L_aK_a\sin(\alpha_1\text{-}\alpha_2) & 0 & -L_bK_a\sin(\alpha_2\text{-}\beta_1) & J_{ab}\sin(\alpha_2\text{-}\beta_2) \\
-L_bK_r\sin(\psi\text{-}\beta_1) & -(J_{ab}\text{-}L_aK_b\text{-}L_bK_a\text{+}L_aL_bM)\sin(\alpha_1\text{-}\beta_1) & L_bK_a\sin(\alpha_2\text{-}\beta_1) & 0 & -L_bK_b\sin(\beta_1\text{-}\beta_2) \\
0 & L_aK_b\sin(\alpha_1\text{-}\beta_2) & -J_{ab}\sin(\alpha_2\text{-}\beta_2) & L_bK_b\sin(\beta_1\text{-}\beta_2) & 0
\end{bmatrix}$$

and

$$C(z) = \begin{bmatrix}
0 & 0 & -1 & -1 & 0 & 0 & 0 & 0 \\
-1 & 0 & 1 & 0 & 0 & 0 & -L_a\cos\alpha_1 & -L_a\sin\alpha_1 \\
0 & -1 & 0 & 1 & 0 & 0 & L_a\cos\alpha_2 & L_a\sin\alpha_2 \\
1 & 0 & 0 & 0 & -1 & 0 & -L_b\cos\beta_1 & -L_b\sin\beta_1 \\
0 & 1 & 0 & 0 & 0 & -1 & L_b\cos\beta_2 & L_b\sin\beta_2
\end{bmatrix}$$

Next, the system is linearized at $\dot{y}_A = \dot{x}_A = 0$; $\dot{y}_E \neq 0$; $\dot{x}_E \neq 0$. If movement $z_i$ and $\dot{z}_l$ are small we can linearize the movement equations around point $z_i = 0$, $\dot{z}_l = 0$, (i = 1, ... ,5). These equations represent the state of equilibrium when $\omega(t) = 0$. This state corresponds to the vertical arrangement of all parts of this mechanism (5-link stands on one leg).

Then, the movement equations are:

$$\ddot{z}_i B_l + gAz_i = C_l \omega \tag{53}$$

From *B(z)* and *C(z)* we can get $B_l$ and $C_l$:

$$B_l = \begin{bmatrix} J & L_a K_r & 0 & L_b K_r & 0 \\ L_a K_r & J_a\text{-}2L_a K_a\text{+}L_a{}^2 M & \text{-}L_a{\cdot}K_a & (J_{ab}\text{-}L_a K_b\text{-}L_b K_a\text{+}L_a L_b M) & \text{-}L_a K_b \\ 0 & \text{-}L_a K_a & J_a & \text{-}L_b K_a & J_{ab} \\ L_b K_r & (J_{ab}\text{-}L_a K_b\text{-}L_b K_a\text{+}L_a L_b M) & \text{-}L_b{\cdot}K_a & J_b\text{-}2L_b K_b\text{+}L_b{}^2 M & \text{-}L_b K_b \\ 0 & \text{-}L_a K_b & J_{ab} & \text{-}L_b K_b & J_b \end{bmatrix}$$

$$C_l = \begin{bmatrix} 0 & 0 & \text{-}1 & \text{-}1 & 0 & 0 & 0 & 0 \\ \text{-}1 & 0 & 1 & 0 & 0 & 0 & \text{-}L_a & \text{-}L_a\alpha_1 \\ 0 & \text{-}1 & 0 & 1 & 0 & 0 & L_a & L_a\alpha_2 \\ 1 & 0 & 0 & 0 & \text{-}1 & 0 & \text{-}L_b & \text{-}L_b\beta_1 \\ 0 & 1 & 0 & 0 & 0 & \text{-}1 & L_b & L_b\beta_2 \end{bmatrix}$$

If $\omega(t) \approx 0$ we can get the linearized motion for 5-link model:

$$B_l \ddot{z}_i + gAz_i = 0 \tag{54}$$

and

$$\ddot{z}_i + gB_l^{-1}Az_i = 0 \tag{55}$$

A boundary value problem for the system (54) or (55) is formulated as follows: find a solution $z(t) = 0$ of the system (54), which at the time $t = 0$ and $t = T$ passes through point $z(0)$ and $z(T)$. We can use the linear non-singular transformation with constant coefficients:

$$z = Rx \tag{56}$$

In normal coordinates at (55) after transformation at (56), we have the form:

$$\ddot{x} + \Omega x = 0 \tag{57}$$

where $\Omega$ is a diagonal 5x5 matrix:

$$\Omega = \begin{bmatrix} \lambda_1 & 0 & 0 & 0 & 0 \\ 0 & \lambda_2 & 0 & 0 & 0 \\ 0 & 0 & \lambda_3 & 0 & 0 \\ 0 & 0 & 0 & \lambda_4 & 0 \\ 0 & 0 & 0 & 0 & \lambda_5 \end{bmatrix},$$

and $\lambda_i$ are roots of characteristic equation:

$$det(B_l\lambda + gA) = 0 \tag{58}$$

Matrix $R$ is known from $B_l$ and $A$:

$$R^T B_l R = E \tag{59}$$
$$R^T gAR = \Omega \tag{60}$$

From the law of inertia of quadratic forms, we have 2 equations:

$$\ddot{x}_i + \omega_i^2 x_i = 0 \ \ (i = 3, 5) \tag{61}$$

and

$$\ddot{x}_i - \omega_i^2 x_i = 0 \ \ (i = 1,2,4) \tag{62}$$

For initial and final conditions:

$$x(0) = R^{-1}z(0) \text{ and } x(T) = R^{-1}z(T) \tag{63}$$

And relationship of these conditions:

$$x_i(t) = \frac{\dot{x}_i(0)}{\omega_i} sin(\omega_i t) + x_i(0) cos(\omega_i t) \tag{64}$$

$$\dot{x}_i(0) = \omega_i \frac{x_i(T) - x_i(0) cos(\omega_i T)}{sin(\omega_i t)} \tag{65}$$

Substitution in (57) we have the final dynamics at joints:

$$x_i(t) = \frac{x_i(T)\,sin(\omega_i T) + x_i(0)\,sin\big(\omega_i(T-t)\big)}{sin(\omega_i t)} \quad (i = 3, 5) \tag{66}$$

and

$$x_i(t) = \frac{x_i(T)\,sh(\omega_i T) + x_i(0)\,sh(\omega_i(T-t))}{sh(\omega_i t)} \quad (i = 1, 2, 4) \tag{67}$$

Equations (66) and (67) are used to test the mathematical model in figure 1 and compared to the experimental data obtained by the real motion capture cameras. Experimental data for real human movement is setup in the next section.

## 3. PRACTICAL DATA COLLECTION

The aim of this study is to create the experimental data for real human movement and compare to the mathematical model. Two motion capture systems: Vicon with markers and Kinet and with marker less, are setup.

### 3.1 Vicon

The Vicon system consists of 10 optical cameras providing the exact movements of markers placed on the body. In this study, 18 markers are placed on the legs into the following positions:
• LHIP (Left HIP) - left hip;
• LKNE (Left KNEe) - left knee;
• LKNI Left Inner KNee) – left inner knee;
• LSHN Left SHIN (lower leg) – left shin;
• RHIP (Right HIP) - right hip;
• RKNE (Right KNEe) – right knee;
• RKNI (Right Inner KNee) – right inner knee;
• RSHN (Right SHiN (lower leg)) – right shin;
• LANK (Left ANKle) - left ankle;
• LHEL (Left HEeL) - left on the heel;
• LMT5 Left 5th MetaTarsal (outside of the foot) - left at the beginning of the little toe;
• LMT1 (Left 1st MetaTarsal (inside of foot)) - left at the beginning of the big toe;
• LTOE (Left TOE (front of the foot)) – left toe;
• RANK (Right ANKle) – right on the ankle;
• RHEL (Right HEeL) - right on the heel;
• RMT5 (Right 5th MetaTarsal (outside of the foot)) – right at the beginning of the little toe;
• RMT1 (Right 1st MetaTarsal (inside of foot)) – right at the beginning of the big toe;
• RTOE (Right TOE (front of the foot)) - right toe.

The Vicon system displays are shown in Figure 2.
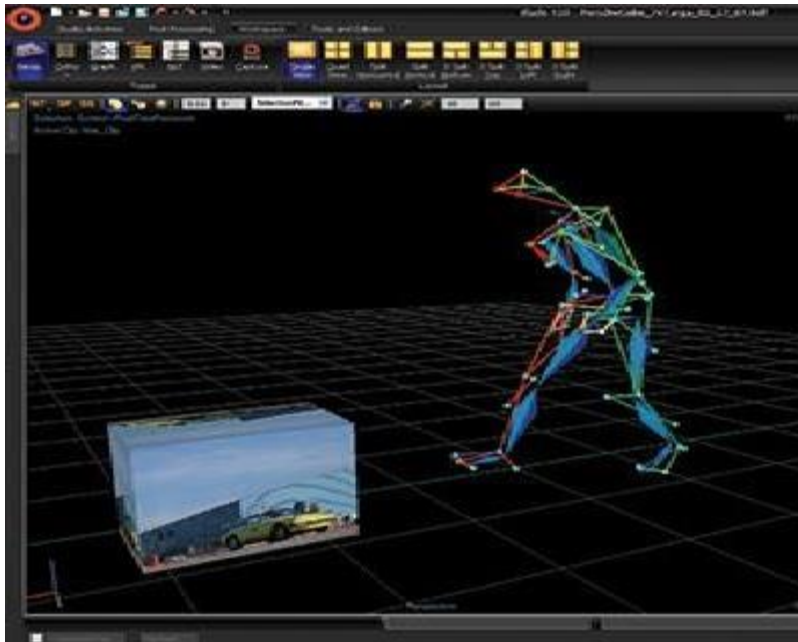
Figure 2. Vicon cameras

The data collection at each markers are saved into the PC as shown in Figure 3.
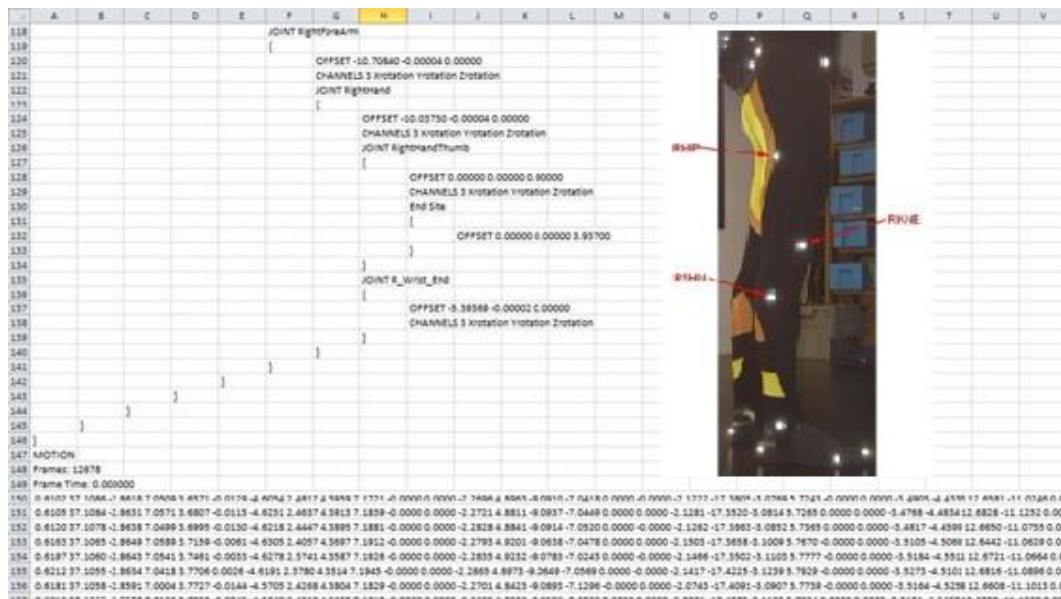


Figure 3. Data collection in Vicon according to markers

## 3.2 Kinect

Another system, that can collect the movement of a human, called Kinect. Kinect is a marker less motion capture system. It collects the human movement from a IR projector emitting the infrared radiation and an infrared receiver for calculating the movements in three dimensional space.

Figure 4 show the motions recording by the Kinect system.

Fig 4. Kinect motion recording

The Kinect will build the skeleton of the human movement as shown in Figure 5.
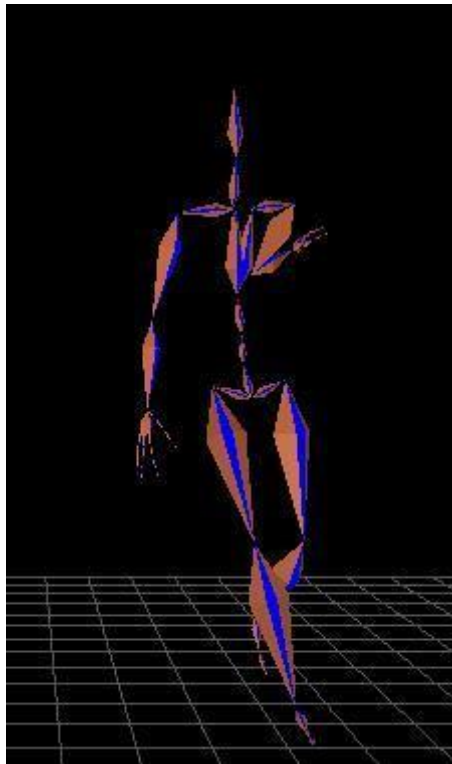


Fig. 5 Skeleton movement in Kinect

## 3.3 Comparison of Vicon and Kinect

From the above two systems, we can see that the Kinect provide bigger errors compared to the Vicon. Figure 5 shows the movement of the knees. The Vicon provides more correctly the knee angles and also smoother movement.
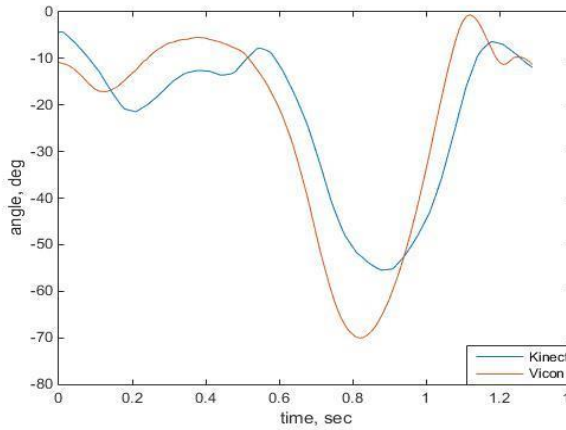
Figure 5.1 right knee
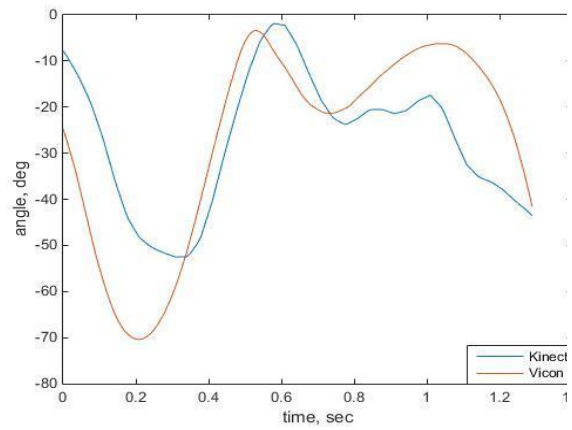


Figure 5.2 left knee

Therefore, in this study, we selected Vicon to record and analyze the real movements and the modeling movements. Figure 6 shows the mathematically modelling movement of a person based on the balanced energy (equation 1 to 67) compared to the experimental data collected from Vicon
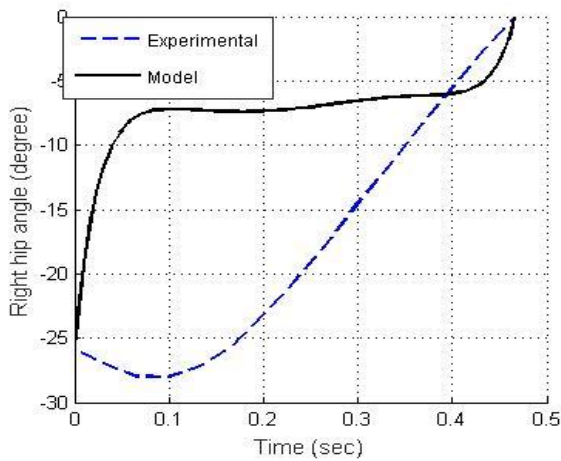


Figure 6.1 Right hip angles
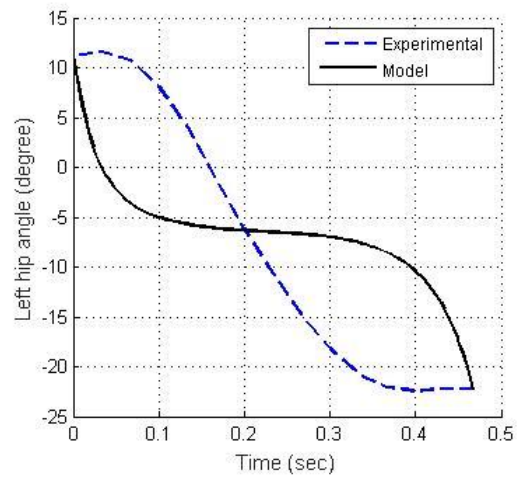


Figure 6.3 Left hip angles
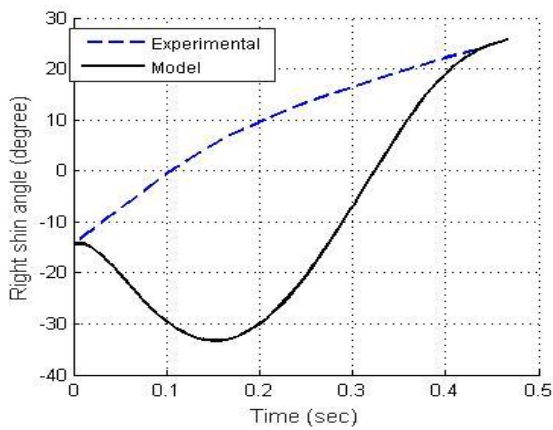


Figure 6.2 Right shin angles
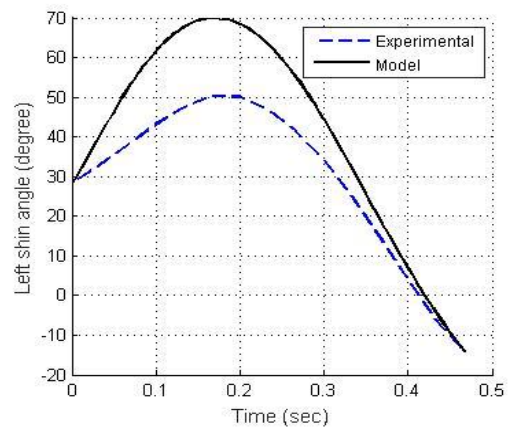


Figure 6.4 Left shin angles

Figure 6. Motions of model vs. experiment

It can be seen that the linearized model leads only to the correct end results. Only the dynamic motions of left shin angles in figure 6.4 are coincided with the experimental data. All other mathematical model trajectories are not similar to the real motions because there is lack of controlled objective function and constraints. Therefore in the next part, we develop MPC as the CNS to generate the optimal torques at each joint and subject to constraints to simulate the human gait motions.

## 4. DESIGN OF MPC

In this paper, the MPC algorithms for nonlinear (NMPC) are referred to in Minh V.T., Rashid A.A., 2012. The general expression for this linearized continuous time in state space is:

$$\dot{x}(t) = \mathbb{A}_C x(t) + \mathbb{B}_C u(t) \tag{68}$$

$$y(t) = \mathbb{C}_C x(t) + \mathbb{D}_C u(t) \tag{69}$$

where $x(t)$ represents the states, $u(t)$ represents the inputs, $y(t)$ represents the output, $\mathbb{A}_C, \mathbb{B}_C, \mathbb{C}_C, \mathbb{D}_C$ are the model state matrices in continuous time.

For computer calculation, the above continuous time system can be discretized (sampling interval $T_0 = 0.01$ sec) as:

$$x(k+1) = \mathbb{A}_D x(k) + \mathbb{B}_D u(k) \tag{70}$$

$$y(k) = \mathbb{C}_D x(k) + \mathbb{D}_D u(k) \tag{71}$$

where $x(k)$ represents the discrete states, $u(k)$ represents the discrete inputs, $y(k)$ represents the discrete output, $\mathbb{A}_D, \mathbb{B}_D, \mathbb{C}_D, \mathbb{D}_D$ are the state matrices in discrete form.

For simplification, we assign the state prediction, $x(k)$, equal to the input prediction horizon, $u(k)$, or $N_{x(k)} = N_{u(k)} = N$ . Then, the objective function of this MPC is:

$$J(x(k), u(k)) = \frac{1}{2} \sum_{k=N_0}^{N-1} [x(k)^T Q x(k) + u(k)^T R u(k)] + \frac{1}{2} x(N)^T Q_f x(N) \tag{72}$$

where $Q$ is the weighting matrix for the predicted states along the prediction horizon, $R$ is the weighting matrix for the control inputs, and $Q_f$ is the weighting matrix for the final predicted states at the final time step. $N$ is the horizon prediction length for both inputs and states.

Constraints for inputs are setup such as the maximum input torques and the limited joint angle at ankles, knees, hips:

$$\min(u(k)) < u(k) < \max(u(k)) \tag{73}$$

Similarly, constraints for states are also setup as:

$$\min(x(k)) < x(k) < \max(x(k)) \tag{74}$$

Example of constraints for hip of a healthy human is illustrated in figure 7.
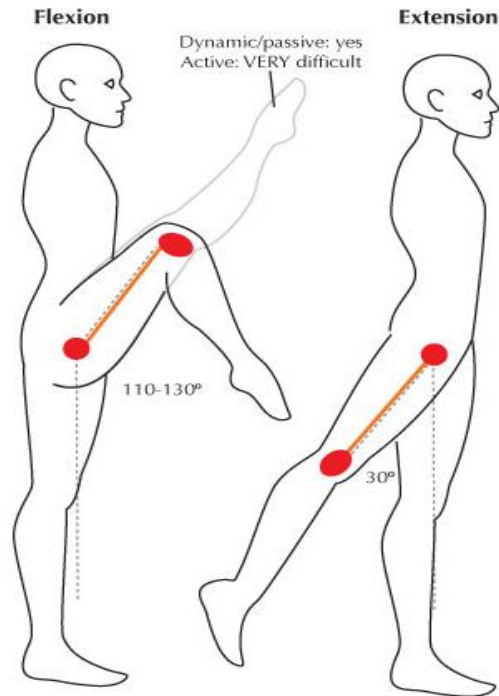
Figure 7. Human hip constrains

For the simplification, we set the horizon prediction length as $N = 50$ for all simulations. A design MPC blocks in Matlab Simulink is developed and shown in figure 8.
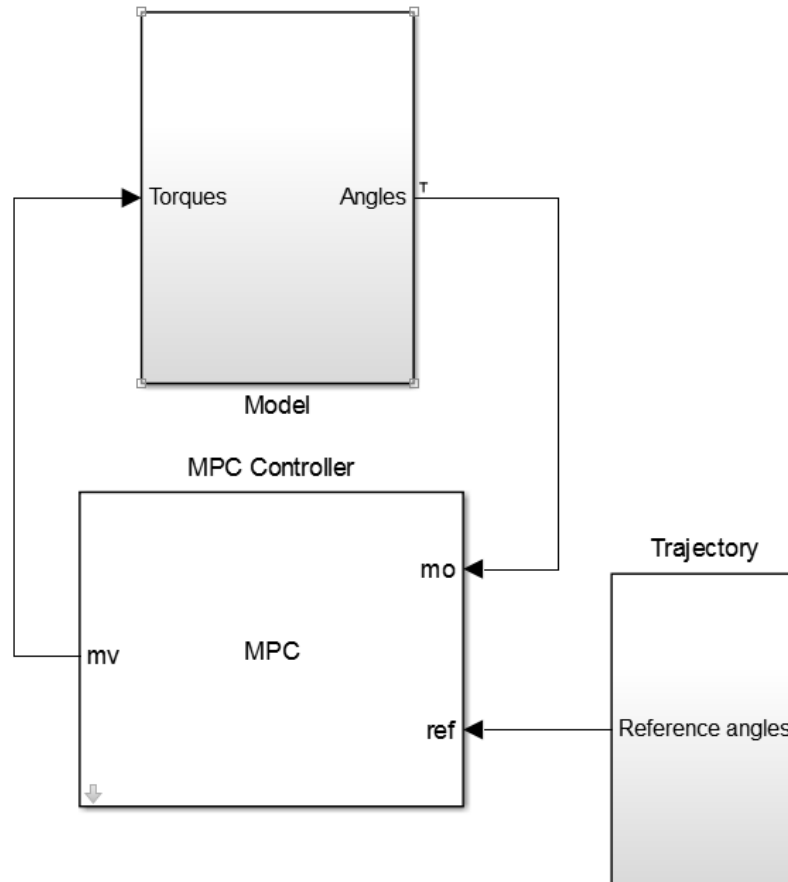


Figure 8. MPC to control the human plant model

MPC designs and calculations are referred in Minh V.T., Afzulpurkar N., 2005 [1] and Minh V.T., Afzulpurkar N., 2006 [10]. This MPC block is used as the internal model to control the external human plant model. The external human plant model is developed and presented in the next part.

## 5. DESIGN OF PLANT MODEL

The model of human plant is designed as five segments including shin, thigh on each side and a hard shell, which replaces the human body above the waist. The same pair of stop - two further segments can be added to the system. This simplification of the 5-link mechanism is taken since the movement of foot has little effect on the general movement of the low weight, and the calculation of the foot rotation considerably complicates our system. The blocks of human plant are developed in Matlab/Simulink and shown in figure 9.
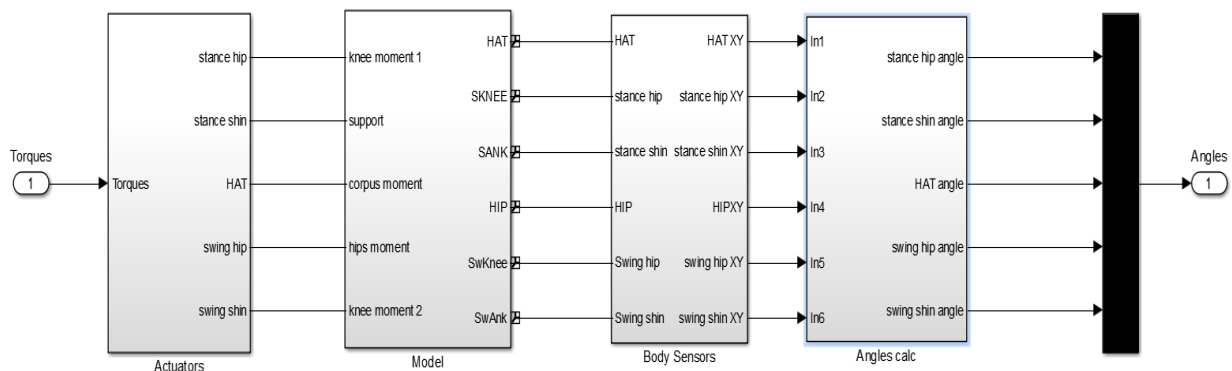


Figure 9. Human plant blocks

The inputs of this plant model are torques, which are supplied to actuators to set the rotation of the block links. The plant model has 5 bodies linked to each other through 4 rotational connections. This plant model describes the movement in one plane only. This simplification is permissible since movement in other planes significantly less. The human plant in Matlab Simulink is shown in figure 10. These mechanical blocks are taken in the library of Matalb Simulink.
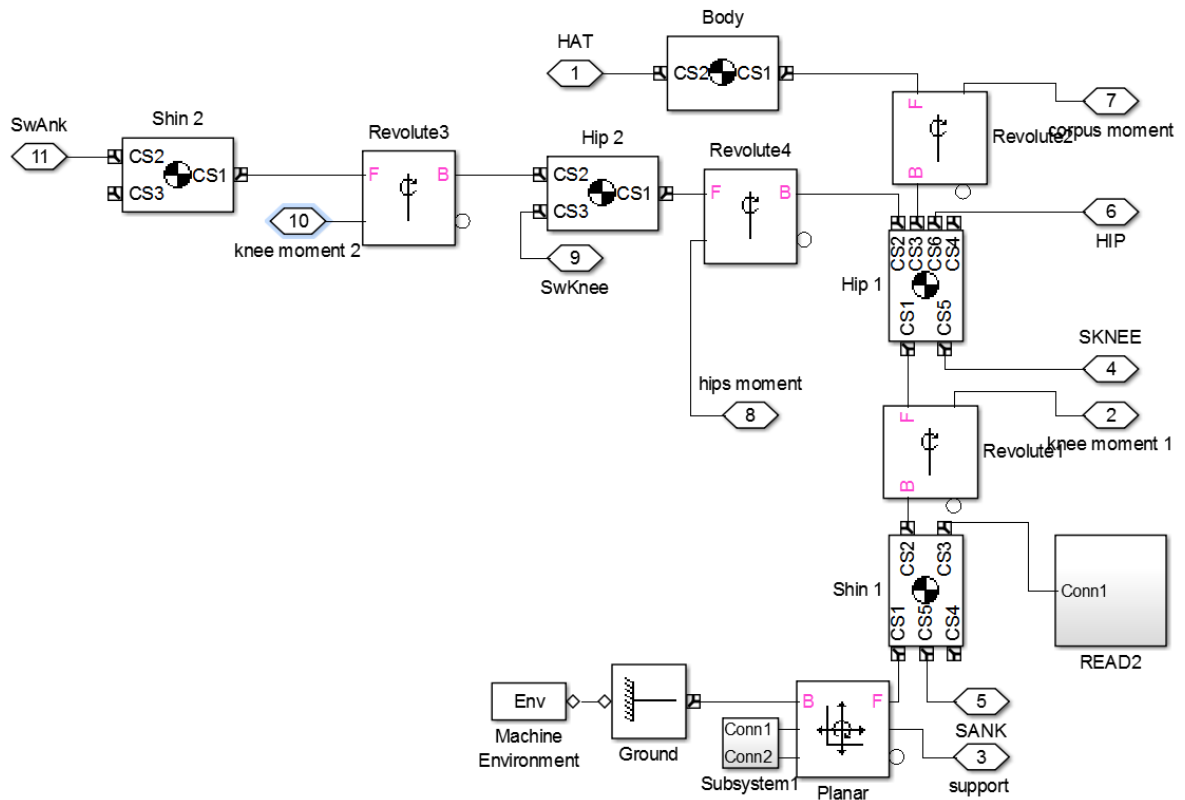
Figure 10. Human mechanical blocks

The above external plant model and the MPC internal model are used to verify the human CNS to perform the human motions. Simulation results are presented in the next part.

## 6. SIMULATION RESULTS

Human gait motions based on MPC are simulated and compared to the experimental data obtained by the motion capture cameras (Vicon) in ITMO University. Mass units, moments of inertia, and the relative location of the centers of mass are estimated by the empirical equation (75) depending on the total mass ($M$) and the human height ($H$). The lengths of the links, the start and end positions are calculated with MPC controller.

$$Y = B_0 + B_1 M + B_2 H \tag{75}$$

where $Y$ – segment mass, $B_0, B_1, B_2$ are coefficients given in table 1

Table 1 Coefficients of mass

| Segment | $B_0$ | $B_1$ | $B_2$ |
|---|---|---|---|
| Shin | $-1.592$ | 0.0362 | 0.0121 |
| Hip | $-2.649$ | 0.1463 | 0.0137 |
| Upper body | 10.3304 | 0.60064 | 0.04256 |

As per Minh V.T., Afzulpurkar N., 2006 [10], the first MPC is tested with zero terminals, $x(N) = 0$. The MPC objective function in (72) becomes:

$$J(x(0), u) = \frac{1}{2} \sum_{k=N_0}^{N-1} [x(k)^T Q x(k) + u(k)^T R u(k)] \tag{76}$$

Simulation results of (76) are shown in figure 11.



Figure 11.1 Sagittal plane right hip angle

Figure 11.3 Sagittal plane left hip angle

Figure 11.2 Sagittal plane right shin angle

Figure 11.4 Sagittal plane left shin angle
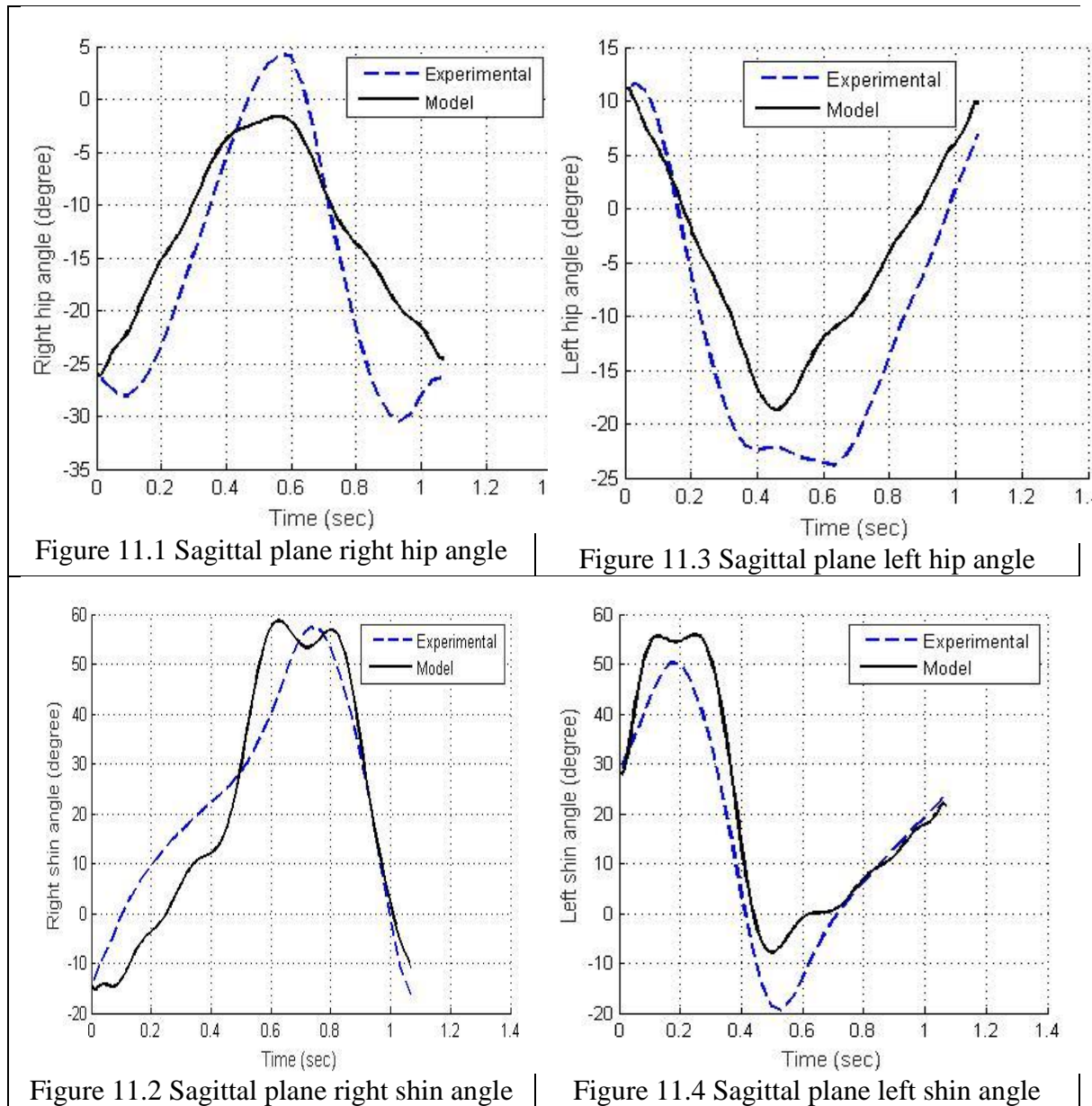
Figure 11. MPC with zero terminals

MPC with zero terminals, $x(N) = 0$, shows that, the models in figure 11.1 and 11.3 do not follow the experimental motions. The model motions in figure 11.2 and 11.4 have two peaks while the real experimental data has only one. Figures from 11.1 to 11.4 show that the mean of angle errors for the right and left hip is 6.2546° and 7.5277°, correspondingly. The mean of angle errors for right and left shin is 8.3327° and 7.9761°, correspondingly.

Next, another MPC controller with softened state constraints is developed:

$$J(x(0), u) = \frac{1}{2} \sum_{k=N_0}^{N-1} [x(k)^T Q x(k) + u(k)^T R u(k)]$$
$$+ \sum_{k=N_0}^{N-1} [\varepsilon(k)^T M \varepsilon(k) + 2\mu(k)^T \varepsilon(k)]$$

(77)

In (77), a penalty term of softened state constraints, $\sum_{k=N_0}^{N-1} [\varepsilon(k)^T M \varepsilon(k) + 2\mu(k)^T \varepsilon(k)]$, is added with a positive definite and symmetric matrix, $M$, and usually large values, $\mu(k)$. These terms help to penalize the violations of the state constraints, as $\varepsilon(k)$ are the state violation values. Simulation results of MPC with softened constraints are shown in figure 12.
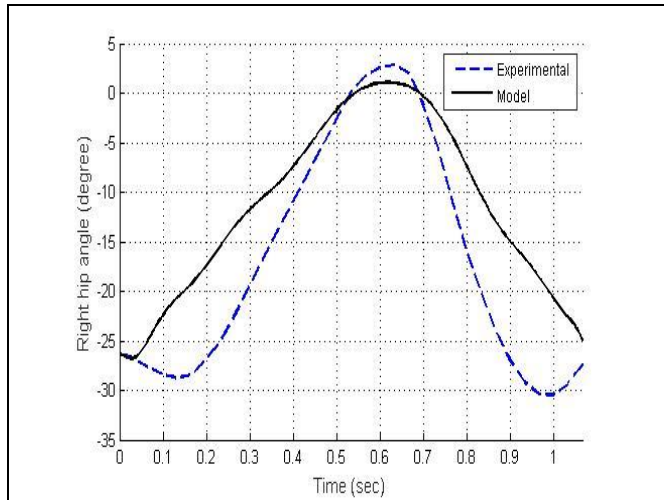


Figure 12.1 Sagittal plane right hip angle
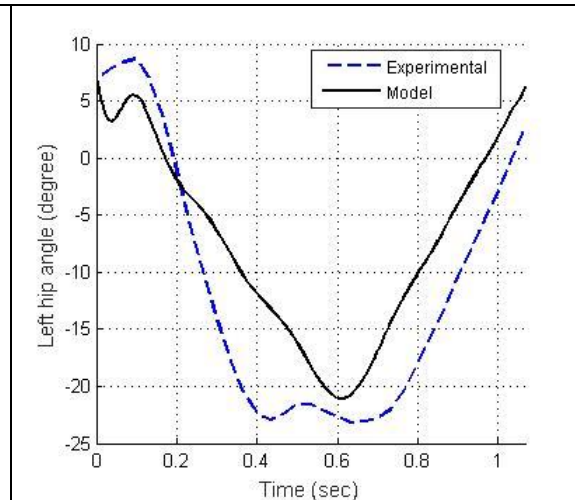
Figure 12.3 Sagittal plane left hip angle
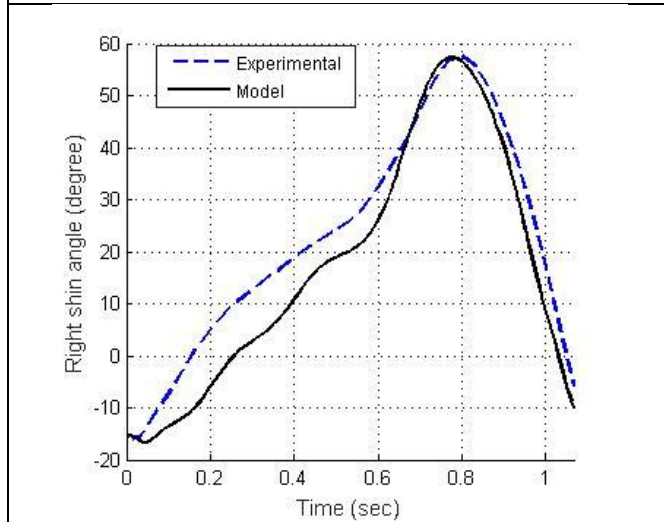
Figure 12.2 Sagittal plane right shin angle
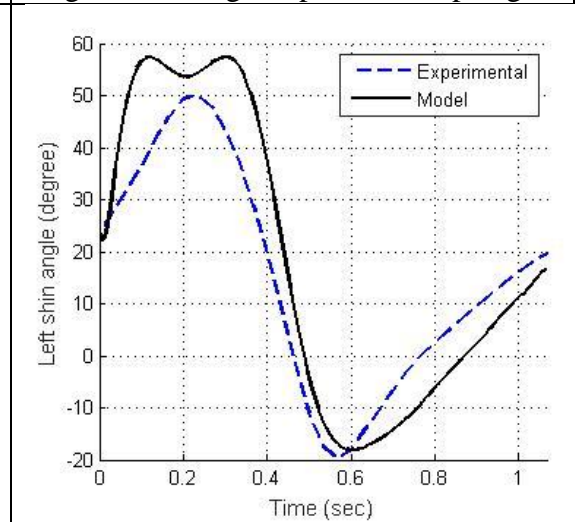
Figure 12.4 Sagittal plane left shin angle

Figure 12. MPC with softened state constraints

Figure 12.1 to 12.4 show that the performances of the MPC with softened state constraints are better than the MPC with zero terminals. The mean of angle errors for the right and left hip is $4.8226°$ and $4.6601°$, correspondingly. The mean of angle errors for the right and left shin is $3.95°$ and $4.145°$. These values are much smaller than the MPC with zero terminals. Therefore, MPC with softened state constraints can be used well to predict the human gait motions. MPC with softened state constraints can

also maintain the stability of the system and always keep the tracking errors at low levels.

## 7. CONCLUSION

We have developed the mathematical model of human gait and MPCs as the CNS to simulate the human motions. Simulation results show that the system is able to generate the kinematic motions of normal persons. Tracking errors are not excessed 5%. The discrepancies can be caused by several reasons: Firstly, the model is highly simplified representation of the human body. Secondly, rotation occurs not only in the sagittal plane but also in the frontal and longitudinal planes. Thirdly, human movement must be considered in three separate intervals - singly, two-supporting and single support on the other foot, otherwise the inevitable errors of the non-equivalence of support. Simulations show that the system with MPC can be used for study of different individual gaits for the diagnosis of diseases and also for autonomous imaging of human gait. Further studies with different MPC algorithms and parameters by varying the weighting matrices, lengths of prediction, constraints are needed to perform in the next phase of this research.

## REFERENCES

[1] Minh V.T., Afzulpurkar N., 2005. Robust model predictive control for input saturated and softened state constraints. Asian Journal of Control, 7(3), 323-329

[2] Vergallo P., Lay-Ekuakille A., Angelillo F., Gallo I., Trabacca A., 2015. Accuracy improvement in gait analysis measurements: Kinematic modeling. In Proc. IEEE Instrumentation and Measurement Technology Conference, Pisa, Italy, 1987-1990

[3] Luengas L.A., Camargo E., Sanchez G., 2015. Modeling and simulation of normal and hemiparetic gait. Frontiers of Mechanical Engineering, 10 (3), 233-241

[4] Gill T., Keller J.M., Anderson D.T., Luke R., 2011. A system for change detection and human recognition in voxel space using the microsoft kinect sensor. In Proc. IEEE Applied Imagery Pattern Recognition Workshop, Washington, USA

[5] Sun J., 2015. Dynamic Modeling of Human Gait Using a Model Predictive Control Approach. PhD thesis, Marquette University

[6 ]Ren L., Howard D., Kenney L., 2006. Computational models to synthesize human walking. Journal of Bionic Engineering, 3, 127-138

[7] Ren L., Jones R., Howard D., 2007. Predictive Modelling of Human Walking over a Complete Gait Cycle. Journal of Biomechanics, 40 (7), 1567–1574

[8] Pontzer H., Holloway J.H., Raichlen D.A., Lieberman D.E., 2009. Control and function of arm swing in human walking and running. Journal of Experimental Biology, 212, 523-534

[9] Mohammed S., Samé A., Oukhellou L., Kong K., Huo W., Amirat Y., 2016. Recognition of gait cycle phases using wearable sensors. Robotics and Autonomous Systems, 75, 50-59

[10] Minh V.T., Afzulpurkar N., 2006. A comparative study on computational schemes for nonlinear model predictive control. Asian Journal of Control, 8(4), 324-331

[11] Minh V.T., Rashid A.A., 2012. Modeling and Model Predictive Control for Hybrid Electric Vehicles. International Journal of Automotive Technology, 13(3), 477-485

[12] Minh V.T, 2011. Conditions for stabilizability of linear switched systems, AIP Conference Proceedings, Vol. 1337 (1), pp. 108-112

[13] Minh V.T and Hashim FBM, 2011. Tracking setpoint robust model predictive control for input saturated and softened state constraints, International Journal of Control, Automation and Systems, vol. 9 (5), pp. 958-965

[14] Minh VT and Afzulpurka N, 2005. Robustness of Model Predictive Control for Ill-Conditioned Distillation Process, Developments in Chemical Engineering and Mineral Processing 13 (3-4), 311-316

[15] Moezzi R, Minh VT, Tamre M, 2018. Fuzzy logic control for a Ball and Beam system, International Journal of Innovative Technology and Interdisciplinary, Vol. 1 (1), pp. 39-48

[16] Minh VT and Khanna R, 2018. Application of Artificial Intelligence in Smart Kitchen, International Journal of Innovative Technology and Interdisciplinary , Vol. 1(1), pp. 1-8

[17] Vu Trieu Minh, Vehicle steering dynamic calculation and simulation, Proceedings of the 23rd International DAAAM Symposium on Intelligent Manufacturing and Automation, Zadar, Croatia, 2012

[18] Vu Trieu Minh, John Pumwa, Modeling and adaptive control simulation for a distillation column, UKSim 14th International Conference on Computer Modelling and Simulation, 2012

[19] VT Minh, D Katushin, M Antonov, R Veinthal, Regression models and fuzzy logic prediction of TBM penetration rate, Open Engineering 7 (1), 60-68, 2017

[20] VT Minh, J Pumwa, International Journal of Control, Automation and Systems 10 (2), 308-316, 2012